Analytical Methods

Accepted Manuscript

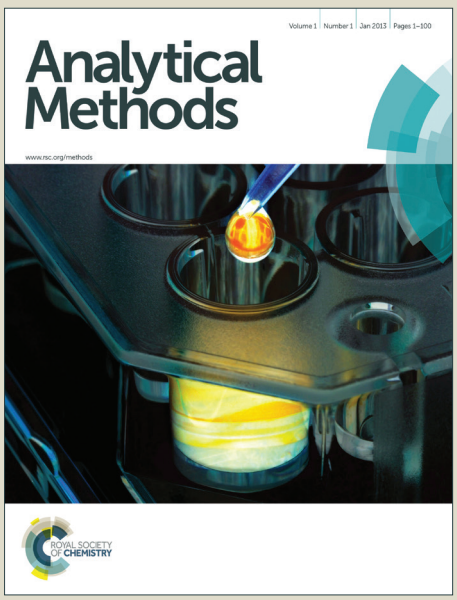

ROYAL SOCIETY OF CHEMISTRY

www.rsc.org/methods

COMMUNICATION

Practical detection for simultaneous analysis of multiple antigens with Staphylococcal protein A as intermediate

Xiaomei Xie, Caiyun Wang, Qian Xiao, Yizhi Zheng, Yuqin Li and Bo Feng*

College of Chemical Engineering, Xiangtan University, Xiangtan 411105, Hunan Province, China

*Corresponding Author. Tel.: +86 731 58298259; Fax: +86 731 58298172.

E-mail address: fengbo@xtu.edu.cn; fengbo5460@hotmail.com

Abstract

Simultaneous measurements of multiple protein biomarkers are typically required to avoid false results in clinical diagnosis. In this work, we present an immunochemical event between antibody and antigen for simultaneous analysis of double biomarkers. In the presence of Staphylococcal protein A (SPA), two kinds of antibodies were captured on the Ni-NTA agarose beads in a site-oriented model. Two target antigens and fluorescence-labeled antibodies were then added in turn to form the immunosorbent complex (antibody-antigen-antibody). The standard sandwich immunoassay can be visualized using a fluorescence microscope to detect the respective fluorescence-labeled antibodies bound to the bead's surface. Meanwhile, a freshly prepared gold-coated substrate was modified with 3-aminopropyl triethoxysilane (APTES) through a glutaraldehyde linker. The immunosorbent complex of the SPA-antibody-antigen was also validated in a quartz crystal microbalance (QCM) apparatus. The results showed an appreciable increase in frequency shift when the SPA, antibody, and antigen bound onto the chip, respectively. Qualitative synchronous fluorescence and quantitative QCM biosensor were practical methods for simultaneous detection of multiple serological antigen biomarkers.

Detection of multiple protein biomarkers is necessary for making an exact diagnosis of disease and providing an effective subsequent treatment in clinical medicine.[1-3] For example, to minimize false-positive and false-negative in cancer diagnosis that can arise from population variations in expression of a single biomarker, simultaneous measurements of a panel of protein biomarkers are required, especially in cases when clinical symptoms are not differentiating.[3-6] And likewise, the levels of these biomarkers at different stages of cancer development have important reference value for the guidance of clinical medication and personalized therapy.[7-9]

To date, most clinical diagnostic assays are conducted using an immobilized antibody as specific probe to determine the target biomarker. Traditional methods for protein biomarkers, such as hepatitis B virus surface antigen (HBsAg) and alpha fetoprotein (AFP), usually involve ELISA (enzyme-linked immunosorbent assay), which based on antigen-antibody specific binding and the enzymatic activity reporter.[10] Recently, quantum dots (QDs) have widely used as the signal probes for the immunoassay based on their narrow emission spectra and highly sensitivity.[11,12] For example, Jun Shen *et al.*[11] combined the advantages of quantum dots with immunochromatographic assay (ICA), which allowed the binding of HBsAg on quantum dot-beads, forming a sandwich ICA platform for ultrasensitive and quantitative detection of HBsAg in human serum. With the rise of nanotechnology, carbon nanotube-based electrochemical biosensors opened a promising approach to evaluate the interaction between antibody and antigen *in vitro*. H. Dai *et al.*[13] introduced a new biosensor based on electrospun carbon nanotubes, wherein AFP antibody was bound to the functionalized electrospun nanofibers for fabricating immunosensor to detect AFP protein.

Simultaneous detection of multiple biomarkers needs different specific antibodies. In mammals, five antibody classes exist, including IgA, IgD, IgE, IgG, and IgM. Fortunately, nearly all antibodies used as probe are from IgG, which is made up of three fragments, namely, two Fab units that can bind specifically to the antigen and another Fc that is identical with the other. Staphylococcal protein A (SPA) can specifically recognize and bind this Fc unit, rendering Fab exposed and accessible to the target analyte, resulting in oriented immobilization of the antibody.[14-17]

The Ni-NTA bead is an affinity chromatography matrix for purifying recombinant proteins carrying a histidine (His) tag. Pull-down assays using Ni-NTA is also an effective tool to study protein–protein interactions.[18] In the current study, we present a

modified method for detection of antigen-antibody interactions using a standard affinity chromatography reagent. Binding events between antigen and antibody, which are traced by fluorescent dye-labeled antibody, are visualized on single affinity chromatography beads by fluorescence microscopy. The use of different fluorescent dyes with different emission wave lengths allows for simultaneous analysis of multiple target biomarkers in a single experiment. However, this method is hard to be adaptable for large-scale setups and quantitative determination because of the fluorescence quenching.

In recent years, quartz crystal microbalance (QCM)-based gravimetric immunosensors with highly sensitive quantitative and real-time detection capabilities have been used extensively. This technology enables the measurement of nanoscale mass and structural changes, thereby offering a robust method for studying molecular interaction. Measurements are based on changes in vibration frequency of a quartz crystal sensor in response to interactions or reactions occurring on the sensor surface. To further optimize the immunosensing performance of the gold electrode and to avoid nonspecific interactions, a more reliable immobilization method for antibody binding to SPA coated gold surface was used in this study.[17,19] A silanization chemistry with 3-aminopropyl triethoxysilane (APTES) is used to attach antibodies to the gold surface with the help of a glutaraldehyde linker,[20-22] which will form a barrier that prevents binding biomolecules from coming in contact with the metal surface.[22] Antibodies are first captured by the SPA immobilized on the electrode surface. Then, the specific antigen attaches to the antibody, and the complex of SPA-antibody-antigen is formed. The frequency shift (Δf) caused by the deposition of proteins on the electrode surface can be related to the adsorbed mass (Δm). The relationship between Δf and Δm is in accordance with the Sauerbrey equation, as follows:

$$\Delta f = \frac{-2 f_0^{\,2} \Delta m}{A\sqrt{\rho_q \mu_q}}$$

where f_0 is the fundamental resonant frequency of the unloaded resonator (f_0=9×10^6 Hz), A is the piezoelectrically active area of the electrodes, and ρ_q and μ_q are the density of quartz (2.648 × 10^3 kg m^{-3}) and the shear modulus (2.947 × 10^{10} kg m^{-1}s^{-2}), respectively.

This study aimed to address a method that can lead to the simultaneous detection

of double antigens (AFP and HBsAg, evaluated as a standard biomarker of liver cancer and hepatitis B, respectively). SPA was used as an intermediate to enhance the site-orientation control rather than random adsorption during antibody immobilization. After immunoreactions, the fluorescence signals of two kinds of fluorescence-labeled antibodies can be obtained simultaneously using a fluorescence microscope. The frequency and mass changes were used for real-time detection by QCM immunosensor. Aside from immunoassay characteristics, surface characterization was also investigated to validate the measurement of multiple protein biomarkers.

Experimental

Materials

Alpha fetoprotein (AFP), anti-AFP antibody, tetramethyl rhodamine isothiocyanate (TRITC)-tagged anti-AFP antibody (Santa Cruz Biotechnology, Inc.), Hepatitis B virus surface antigen (HBsAg), anti-Hepatitis B virus surface antigen antibody (HBsAb), and fluorescein isothiocyannate (FITC)-tagged HBsAb (Biorbyt, Cambridge, UK) were used throughout the study. SPA and His-SPA were purchased from Axxora (San Diego, USA). Ni-NTA agarose beads (size: 45-165 μm) were purchased from Qiagen. Acetone (AR) and absolute ethanol (AR) were purchased from Xiangke Fine Chemical Factory (China). Concentrated sulfuric acid (98%) and hydrogen peroxide (30%) were provided by Xing Kong Chemical Glass Co., Ltd. (China). The organosilane reagent 3-aminopropyl triethoxysilane (APTES) and the linker glutaraldehyde (GA), with solutions of 5% APTES in acetone and 5% glutaraldehyde in Milli-Q water, respectively, were obtained from Sigma-Aldrich. Phosphate-buffered saline (PBS, 10 mM, pH 7.2) was sterilized, preserved at 4 °C, and used as a wash and dilution buffer. SPAs in the PBS solution were deployed at 1 mg/ml. All antibodies were diluted with PBS solution into 1 mg/ml and stored at 4 °C separately. A blocking buffer was prepared by dissolving bovine serum albumin (BSA, Sigma Aldrich) in the PBS solution (containing 0.1% BSA). A washing buffer was prepared by adding Tween-20 to the PBS solution (containing 0.05% Tween-20).

Fluorescence microscope

Ni-NTA beads were washed thrice with PBS buffer for 3 min at 400 r/min, and the supernatant was then discarded. The Ni-NTA beads were incubated with 500 μl of 50 μg/ml His-SPA solution for 12 h at 4 °C. After incubation, the beads were washed thrice with PBS solutions for 3 min at 400 r/min to remove the unreacted His-SPA.

Afterward, the beads were incubated in 0.1% BSA solution (in PBS) with shocking for 4 h at 4 °C to block all available nonspecific binding sites, and then washed with PBS buffer to remove excess BSA. Second, Ni-NTA beads covered with His-SPA were immersed in 0.1 mg/ml antibody solutions with oscillation for 6 h at 4 °C. The beads were then incubated in antigen solutions with shocking for 6 h at 4 °C. Finally, the beads were immersed in fluorescence-labeled antibodies in the dark with shocking for 6 h at 4 °C. The samples after each step were rinsed by washing buffer thrice to remove the nonspecific adsorbed proteins. A cross-over experiment was then conducted following the same steps listed above, but using different fluorescence-labeled antibodies. The beads were stored in the dark at 4 °C until scanning.

A fluorescence microscope (MF30, Mshot Company) was used to capture the images of fluorescent signal emitted by labeled biomolecules bound to the beads. A filter system was used for blue excitation (excitation wavelength: 480 ± 40 nm) of FITC-tagged biomolecules and green excitation (excitation wavelength: 527 ± 30 nm) of TRITC-tagged complexes, which in turn emitted the green fluorescence and the red fluorescence, respectively.

Quartz crystal microbalance (QCM)

The QCM crystal was rinsed with acetone in an ultrasonic bath for 5 min and then washed with Milli-Q water. Afterward, the QCM crystal was dried in an N_2 gas stream, followed by absolute ethanol, before coating. To remove any organic contamination from the crystal surface and to improve the hydrophilic nature of the freshly prepared gold surface, the chip was treated by dipping into piranha solution (98% H_2SO_4/30% H_2O_2, 7:3 in v/v) for 5 min. Piranha solution has strong corrosive properties; great care should be taken to avoid any contact with the electrode welding points. After rinsing thoroughly with Milli-Q water and drying with nitrogen, the chip surface was hydrophilic. A 5% APTES solution in acetone was immediately added to the crystal surface for 1 h at room temperature. Afterward, the sample was rinsed with Milli-Q water and blown dry under a stream of N_2. The chip was placed in a 5% glutaraldehyde solution for 3 h to allow cross linking between the chip and the SPA.

Frequency shift was monitored and recorded in liquid media at room temperature. Previous experiments demonstrated that no significant shift of frequency occurred after adding 50 μg/ml of SPA solution prepared in PBS, thereby indicating the saturation of GA-(APTES)-modified quartz crystal with SPA solution at 50 μg/ml

protein concentration. This concentration was selected for all the subsequent experiments thereafter. After the baseline obtained with PBS was stabilized, it was rinsed with a buffer solution. When the frequency was stable, the QCM biosensor was prepared for incubation in 0.1% BSA solution. After covering with BSA, the chip blocked all available nonspecific binding sites that were not bound to the SPA on the modified chip. The chip was then rinsed with PBS to wash off excess BSA. When the frequency was stable, anti-AFP antibody (100 μg/ml) and HBsAb (100 μg/ml) were added to the activated QCM crystal and rinsed with PBS buffer when the frequency was stable. Only a small difference in frequency shift was observed between the antibody concentrations (0.01-1 mg/ml). The concentration of the antibody was optimized to 100 μg/ml and then used for all subsequent experiments. A drop of AFP protein (100 μg/ml) was introduced to the cell to measure the binding of the anti-AFP antibody onto the SPA-coated surface, after which rinsing was done with PBS buffer. Finally, HBsAg (100 μg/ml) was added to the chip surface to verify the binding of HBsAb onto the chip surface; excess HBsAg was removed by rinsing with PBS buffer. For each adsorption step, the same buffer (PBS solution) was flushed through the chamber to remove the non-covalently bonded proteins; a QCM immunosensor was prepared for detection. In the final step, the "sandwich" (SPA-antibody-antigen) complex was formed, which was attached to the sensor surface. The process is illustrated in Fig. 1. Measurements were conducted until a stable frequency (frequency shift less than 3 Hz) was observed for >1 min. The amount of protein bound to chip surface was determined with a QCM.

A QCM (Maxtek, USA) with 9 MHz AT-cut quartz crystals (gold coated) was used to quantitatively study the ability of proteins to bind to the chip. The gold surface had a surface area for immobilization of 1.37 cm^2. With the same protocol, the proteins were linked on the QCM surface, and the mass sensitivity of the crystal was calculated as 0.012 Hz/ng/cm^2.

Atomic Force Microscopy (AFM)

AFM experiments were performed with atomic force microscope Agilent 5500. For AFM studies, silicon substrates were prepared with the same modification techniques as those described above for the QCM chips. Biomolecular imaging was conducted in non-contact mode in air at room temperature. The AFM images were analyzed using image processing software to calculate the root-mean-square roughness value and maximum height (Rmax). The average surface roughness (Ra) for each AFM image

was calculated using the PicoView^{R} software package provided with the instrument.

Results and discussion

Fluorescence imaging

His-SPA molecules were first immobilized on Ni-NTA agarose gel beads to prevent random immobilization of the antibodies. Meanwhile, standard sandwich immunoassay (antibody-antigen-antibody) was used on His-SPA coated Ni-NTA beads. The existence of fluorescence confirmed the presence of respective immune complexes on the beads surface. In this study, simultaneous detection of two kinds of fluorescence-labeled antibodies can be realized by measuring the fluorescence signals.

Anti-AFP antibody labeled with TRITC exhibited appeared red light through green light irradiation. In the presence of FITC-tagged HBsAb, green light was obtained by measuring the blue light excitation spectra. The fluorescence images of the two kinds of immune complexes are presented in Fig. 2. The existence of the circular green regions was testified by the immunoreactions of the FITC-conjugated HBsAb and HBsAg on the Ni-NTA beads, whereas the circular red regions were confirmed by the immune reactions of the TRITC-conjugated anti-AFP antibody. As shown in Fig. 2A and 2B, circular red and circular green regions were present on each single bead. Fluorescence images demonstrated that the Ni-NTA beads both integrated with anti-AFP antibodies, but also combined with HBsAb. According to Fig. 2B, the Ni-NTA beads without His-SPA also combined with anti-AFP antibody and HBsAb. However, the fluorescence intensity of the beads decreased in the absence of His-SPA. As shown in Fig. 2C, after the Ni-NTA beads were blocked with BSA, the circular red and circular green regions were hardly observed, suggesting two kinds of immunocomplexes were not adsorbed on the beads.

As a control in the cross-over experiment, the fluorescence-labeled antibody specifically bound to the Ni-NTA beads (Fig. 3). As shown in Fig. 3A and 3B, the Ni-NTA beads emitted only one kind of fluorescence excited by light when the fluorescence-labeled antibody bound to its specific antigen. It indicates that there is no cross-reaction between antigens and antibodies. Fluorescence microscope is a feasible tool for simultaneously detection of multiple biomarkers.

Furthermore, this approach was applied to diagnose double antigen biomarkers in actual human serum samples, and the results were compared with commercial ELISA kits. Densitometric analysis of the circular red/green regions was performed

with the software ImageJ 1.43m. Quantitative data based on the measurement of mean intensity inside the circle were presented in Table 1. It shows that the proposal method of synchronous fluorescence has acceptable and accurate results compared to the AFP/HBsAg ELISA kit (AutoBio Diagnostics, China) in the detection of 12 serum samples (4#, 5# and 6# containing analytes of both AFP and HBsAg). The LOD (limit of detection, defined as the analyte concentration that is required to produce a signal greater than three times of normal human serum value) of synchronous fluorescence is found to be 0.5 and 0.2 ng/ml when detecting AFP and HBsAg respectively. In contrast, the LOD of assay using AFP/HBsAg ELISA kit is just 2.5/0.5 ng/ml.

Quartz crystal microbalance (QCM)

The first immunoreaction occurred between SPA and antibody. SPA was immobilized first on the chips to prevent the random immobilization of the antibodies. The chips were subjected to an acidic treatment, followed by aqueous silanization, to increase surface hydrophilicity, which would increase the ability to add functional groups. The gold surface was then blocked by 0.1% BSA solution. The mixed solution of anti-AFP antibody and HBsAb was added and reacted with the SPA-coated surface. After antibody immobilization, the antigen solution was linked to the antibody. The typical frequency changes of the quartz crystal functionalized with SPA as a result of a cascade of interactions with antibodies and antigens are shown in Fig. 4. Point 1 refers to when SPA solution (50 μg/ml) was allowed to react with the GA-APTES-modified quartz crystal. The signal became stable only after 20 min. Point 2 indicates the event wherein the crystal was subjected to several wash cycles. Point 3 was the time at which the frequency of the crystal stabilized when all non-specifically adsorbed molecules were rinsed away, and SPA was specifically bound on the surface. After SPA binding step, 0.1% BSA solution was supposed to block any non-specific binding (point 3) because it showed low affinities for antibodies. Point 4 was when the solution comprising a mixture of anti-AFP antibody and HBsAb was added to the crystal. The binding of the antibody to the immobilized SPA caused a decrease in the resonant frequency, and stabilization occurred after 30 min. Point 5 corresponds to the final resonant frequency after rinsing with PBS solution. The frequency shift for antibody immobilization was found at 96.6 Hz. Point 5 refers to the time when anti-AFP antigen solutions (100 μg/ml) were added to the chip surface. The frequency shift was 47.1 Hz (point 6). For the final step, 100 μg/ml HBsAg solution in PBS was added, and after successive additions, the final frequency shift was 47.9 Hz (point 6).

These results indicated that two kinds of antibodies can simultaneously be immobilized on the chip, and the antigen is not cross-reactive with the antibody. According to the Sauerbrey relation, the adsorption amount of anti-AFP antibody and HBsAb was calculated as 2.86 μg and 2.91 μg, respectively. The QCM sensor revealed that using SPA as an intermediate for site-oriented immobilization can accomplish simultaneous detection.

AFM

To obtain quantitative impression and estimate the uniformity of the surface morphology, AFM topographies of three substrates were obtained, as follows: APTES-modified crystal (Fig. 5A), SPA-coated crystal (Fig. 5B), and APTES + SPA modified crystal. The AFM image of the APTES-modified crystal was affected by the amount of crosslinking agent glutaraldehyde solution, as shown in Fig. 5A, which is different from that in Fig. 5B and 5C. In comparison, the AFM topography of the SPA-coated crystal surface (Fig. 5B) revealed that the gold-coated quartz crystals showed a relatively smooth surface. The orientation of the SPA molecules is not uniform. Hence, the active sites on one protein molecule may sterically hinder the active sites on the other, resulting in a non-uniform binding of biomolecules and loss of active sites. More active sites for antibody immobilization can result in improved binding and higher sensitivity. The film in Fig. 5C was more uniform, with a maximum height (R_{max}) of 200 nm, compared with the one shown in Fig. 5B. Thus, these two approaches can be combined in such a way that the antibodies can be immobilized on the crystal surface uniformly.

Conclusions

In this study, an *in vitro* detection method for simultaneous analysis of double antigen biomarkers was presented and validated by the results obtained via fluorescence microscopy and QCM biosensor in the presence of SPA. SPA acted as the control unit to achieve oriented immobilization of the capture antibody. The AFM surface morphology study revealed improvement in the roughness of the surface on which the biomolecules were immobilized. Currently, rapid, sensitive, and simultaneous detection of multiple biomarkers in complex biological samples is still a challenge for clinical diagnostics.[23-26] Integration of advances in oriented interfacial adsorption and surface modification would offer a unique idea as a way to fabricate detection devices. Those high-throughput, large-scale platforms, such as micro- or nano-chips, allow

parallel detection of thousands of addressable elements in a single experiment, are too expensive and technically complex for routine clinical diagnostics.[6,27-29] Alternatively, most laboratories are capable of performing fluorescent microscopy or QCM easy and convenient, the methods proposed in this paper can be taken as a practical supplement of multiple-target analysis.

Acknowledgements

This work was supported by National Natural Science Foundation of China (31270988, 21306161), Undergraduate Innovational Experimentation Program of Xiangtan University (2014xtuxj40), Scientific Research Fund of Hunan Provincial Education Department (13B120), China Postdoctoral Science Foundation (2014M562118) and Hunan Provincial Natural Science Foundation of China (2015JJ2133).

References

1 H. Mukundan, H. Xie, D. Price, J. Z. Kubicek-Sutherland, W. K. Grace, A. S. Anderson, J. S. Martinez, N. Hartman and B. I. Swanson, *Anal. Chem.*, 2010, 82, 136-144.

2 J. M. Lee, J. J. Han, G. Altwerger and E. C. Kohn, *J. Proteomics*, 2011, 74, 2632-2641.

3 B. V. Chikkaveeraiah, A. A. Bhirde, N. Y. Morgan, H. S. Eden and X. Chen, *ACS Nano*, 2012, 6, 6546-6561.

4 J. D. Wulfkuhle, L. A. Liotta and E. F. Petricoin, *Nat. Rev. Cancer*, 2003, 3, 267-275.

5 V. Kulasingam and E. P. Diamandis, *Nat. Clin. Pract. Oncol.*, 2008, 5, 588-599.

6 J. F. Rusling, C. V. Kumar, J. S. Gutkind and V. Patel, *Analyst*, 2010, 135, 2496-2511.

7 J. A. Ludwig and J. N. Weinstein, *Nat. Rev. Cancer*, 2005, 5, 845-856.

8 M. Ferrari, *Nat. Rev. Cancer*, 2005, 5, 161-171.

9 S. F. Kingsmore, *Nat. Rev. Drug. Discov.*, 2006, 5, 310-320.

10 R. Wei, G. J. Knight, D. H. Zimmerman and H. E. Bond, *Clin. Chem.*, 1977, 23, 813-815.

11 J. Shen, Y. Zhou, F. Fu, H. Xu, J. Lv, Y. Xiong and A. Wang, *Talanta*, 2015, 142, 145-149.

12 R. Xu, Y. Jiang, L. Xia, T. Zhang, L. Xu, S. Zhang, D. Liu and H. Song, *Biosens. Bioelectron.*, 2015, 74, 411-417.

13 H. Dai, G. Xu, S. Zhang, L. Gong, X. Li, C. Yang, Y. Lin, J. Chen and G. Chen, *Biosens. Bioelectron.*, 2014, 61, 575-578.

14 K. Nakanishi, T. Sakiyama, Y. Kumada, K. Imamura and H. Imanaka, *Curr. Proteom.*, 2008, 5, 161-175.

15 B. Feng, C. Wang, X. Xie, X. Feng, Y. Li and Z. Cao, *Biochem. Biophys. Res. Commun.*, 2014, 450, 429-432.

16 A. Makaraviciute and A. Ramanaviciene, *Biosens. Bioelectron.*, 2013, 50, 460-471.

17 M. Iijima, H. Kadoya, S. Hatahira, S. Hiramatsu, G. Jung, A. Martin, J. Quinn, J. Jung, S. Y. Jeong, E. K. Choi, T. Arakawa, F. Hinako, M. Kusunoki, N. Yoshimoto, T. Niimi, K. Tanizawa and S. Kuroda, *Biomaterials*, 2011, 32, 1455-1464.

18 A. Kaushansky, J. E. Allen, A. Gordus, M. A. Stiffler, E. S. Karp, B. H. Chang and G. MacBeath, *Nat. Protoc.*, 2010, 5, 773-790.

19 J. Zhou, L. Du, L. Zou, Y. Zou, N. Hu and P. Wang, *Sens. Actuators B Chem.*, 2014, 197, 220-227.

20 M. J. Oliver, J. Hernando-García, P. Pobedinskas, K. Haenen, A. Ríos and J. L. Sánchez-Rojas, *Colloids Surf. B Biointerfaces*, 2011, 88, 191-195.

21 D. Matatagui, J. Fontecha, M. J. Fernández, M. J. Oliver, J. Hernando-García, J. L. Sánchez-Rojas, I. Gràcia, C. Cané, J. P. Santos and M. C. Horrillo, *Sens. Actuators B Chem.*, 2013, 189, 123-129.

22 N. S. K. Gunda, M. Singh, L. Norman, K. Kaur and S. K. Mitra, *Appl. Surf. Sci.*, 2014, 305, 522-530.

23 G. J. Zhang, Z. H. Luo, M. J. Huang, J. J. Ang, T. G. Kang and H. Ji, *Biosens. Bioelectron.*, 2011, 28, 459-463.

24 H. C. Tekin and M. A. Gijs, *Lab Chip*, 2013, 13, 4711-4739.

25 B. A. Otieno, C. E. Krause, A. Latus, B. V. Chikkaveeraiah, R. C. Faria and J. F. Rusling, *Biosens. Bioelectron.*, 2014, 53, 268-274.

26 L. Xiong, L. Gao, Q. Liu, J. Xia, X. Han and Y. Liu, *Anal. Methods*, 2013, 5, 2413-2418.

27 S. Baratchi, K. Khoshmanesh, C. Sacristán, D. Depoil, D. Wlodkowic, P. McIntyre and A. Mitchell, *Biotechnol. Adv.*, 2014, 32, 333-346.

28 S. A. Svarovsky and L. Joshi, *Anal. Methods*, 2014, 6, 3918-3936.

29 S. J. Maerkl, *Curr. Opin. Biotechnol.*, 2011, 22, 59-65.

Table 1. Evaluation and comparison of synchronous fluorescence with traditional ELISA in serodiagnosis

Method	Analyte	AFP (+)			AFP (+)/HBsAg (+)			HBsAg (+)			Normal human serum			LOD ng/ml
		1#	2#	3#	4#	5#	6#	7#	8#	9#	10#	11#	12#	
Synchronous fluorescence [a] (Mean Dens)	AFP	150	173	198	242	250	207	12.2	10.5	14.3	8.07	7.58	9.13	0.5
	HBsAg	12.8	10.5	7.40	255	239	248	213	245	255	6.97	10.4	8.61	0.2
Traditional ELISA [b] (Mean A_{450})	AFP	0.35	0.54	0.71	1.24	1.38	0.76	0.02	0.01	0.01	0.02	0.01	0.02	2.5
	HBsAg	0.02	0.02	0.01	1.68	1.25	1.34	0.72	1.39	1.66	0.00	0.01	0.01	0.5

[a] The resulting images were loaded into the software ImageJ 1.43m and transformed into 8-bit color ones (Image→Color→Split channels). The 8-bit red and green fluorescent-channel images were then ready for further quantification. A circle enclosing the Ni-NTA bead in the brightfield image was drawn by using the "Elliptical selection" tool. The average intensity inside the circle (expressed as Mean Dens) was measured image by image (Analyze→Measure). [b] ELISA protocol: 50 μl serum sample and 50 μl horseradish peroxidase-conjugated anti-AFP/ anti-HBs were added to each well of microplates. After 30 min incubation at 37 °C, the plates were washed to remove any unbound conjugate and developed with the substrate tetramethylbenzidine for 5 min. The colorimetric reaction was terminated by addition of 50 μl of 2 M H_2SO_4 and absorbance value was measured at 450 nm by using a model 550 microplate reader (Bio-Rad, USA). All tests were repeated four times and the arithmetic mean of absorbance values (A_{450}) was presented. 12 representative serum samples (4#, 5# and 6# containing analytes of both AFP and HBsAg) were obtained from National Institute for the Control of Pharmaceutical and Biological Products (Beijing, China). The LOD (limit of detection) is defined as the analyte concentration that is required to produce a signal greater than three times of normal human serum value.

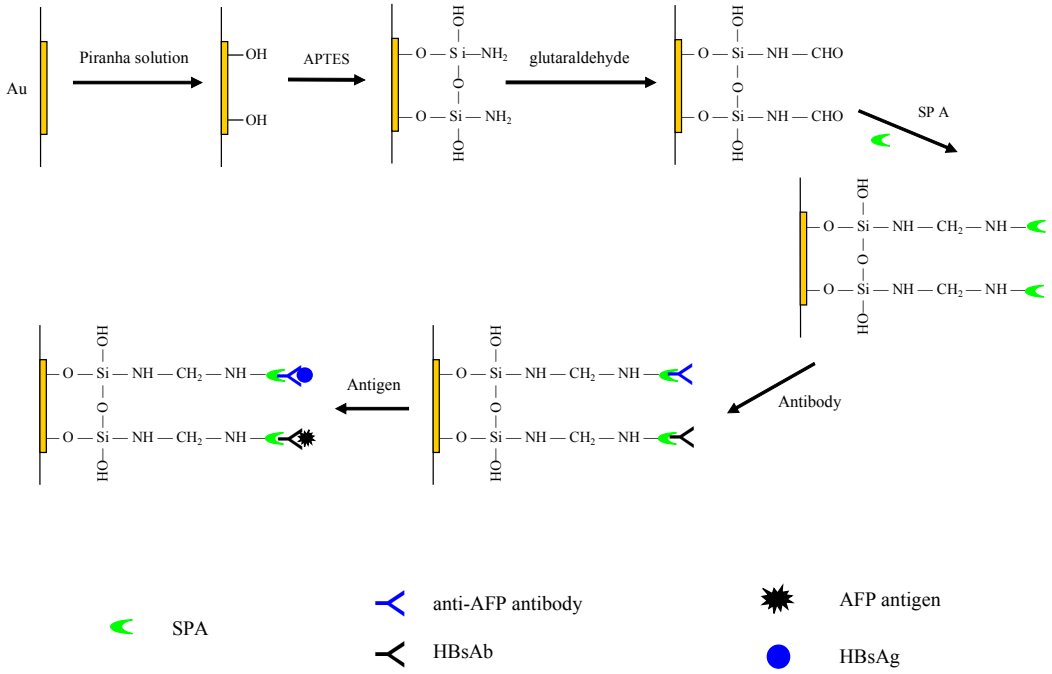

Fig. 1 Schematic of the site-oriented immobilization of antibodies onto the chip surface using SPA as an intermediate. The experimental procedures involves: a) substrate cleaning (piranha cleaning); b) treatment with APTES (5%) and glutaraldehyde (5%) solutions; c) immobilization of capture antibodies; and d) immobilization of antigen biomolecules.

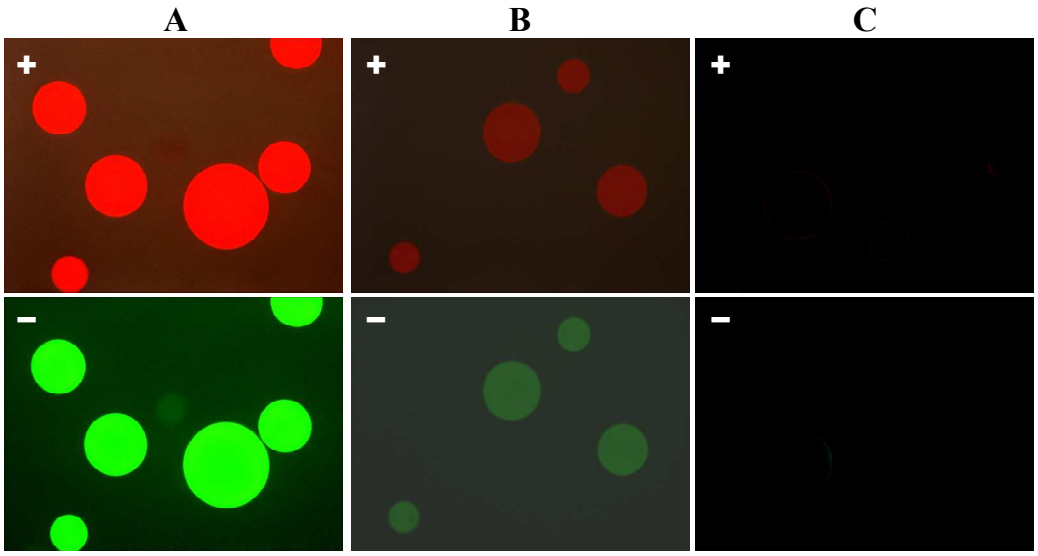

Fig. 2 Fluorescence images of the Ni-NTA agarose beads were obtained by FL microscopy, with green light (+) and blue light (−) excitation spectra. The beads were integrated with two kinds of immunocomplexes, as follows: (A) both anti-AFP antibody and HBsAb integrated with fluorescence-labeled specific secondary antibodies blocked with BSA in the presence of His-SPA; (B) both anti-AFP antibody and HBsAb integrated with fluorescence-labeled specific secondary antibodies blocked with BSA in the absence of His-SPA; (C) Ni-NTA beads were blocked with BSA, then both anti-AFP antibody and HBsAb integrated with fluorescence-labeled specific secondary antibodies were incubated with beads in the presence of His-SPA.

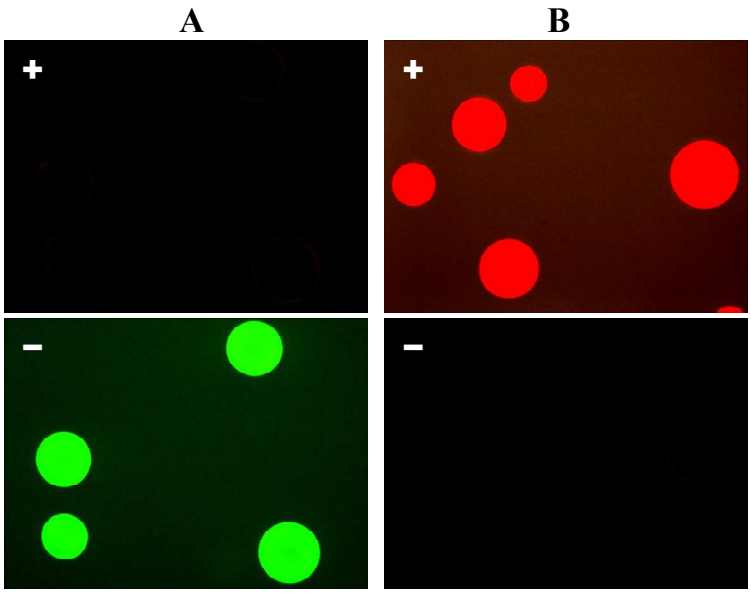

Fig. 3 Fluorescence images of Ni-NTA agarose beads were obtained by FL microscopy, with green light (+) and blue light (−) excitation spectra in the cross-over experiment. The beads were integrated together with (A) HBsAb, HBsAg, and FITC-conjugated HBsAb, along with TRITC-conjugated anti-AFP antibody; (B) anti-AFP antibody, AFP protein, and TRITC-conjugated anti-AFP antibody, along with FITC-conjugated HBsAb.

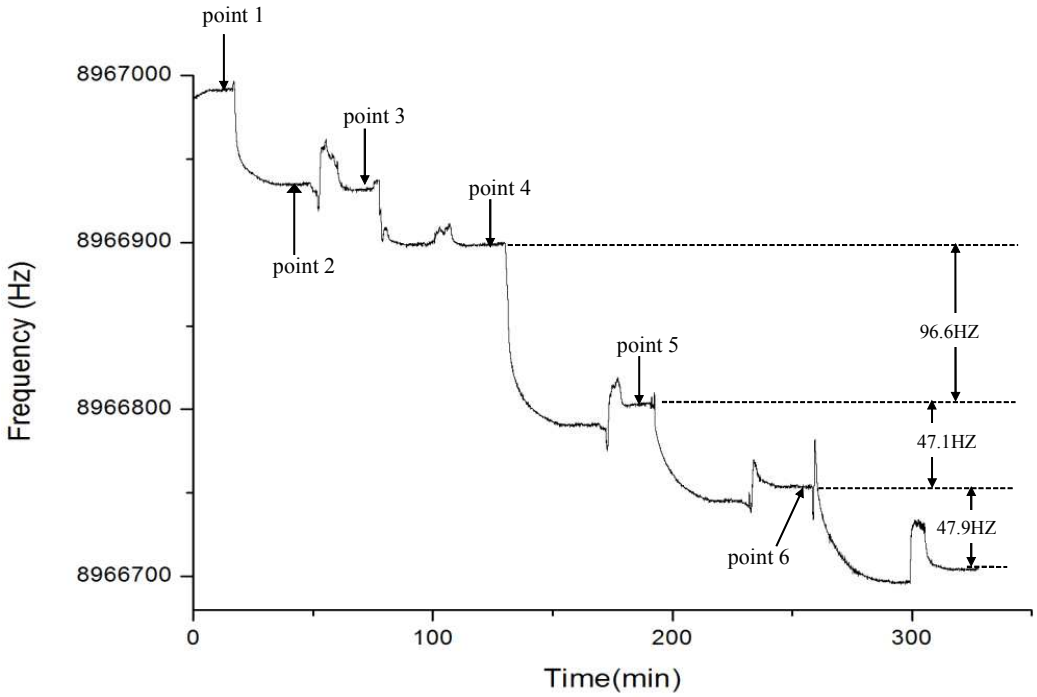

Fig. 4 QCM frequency responses for the addition of specific antibodies and antigens to the SPA modified quartz crystal.

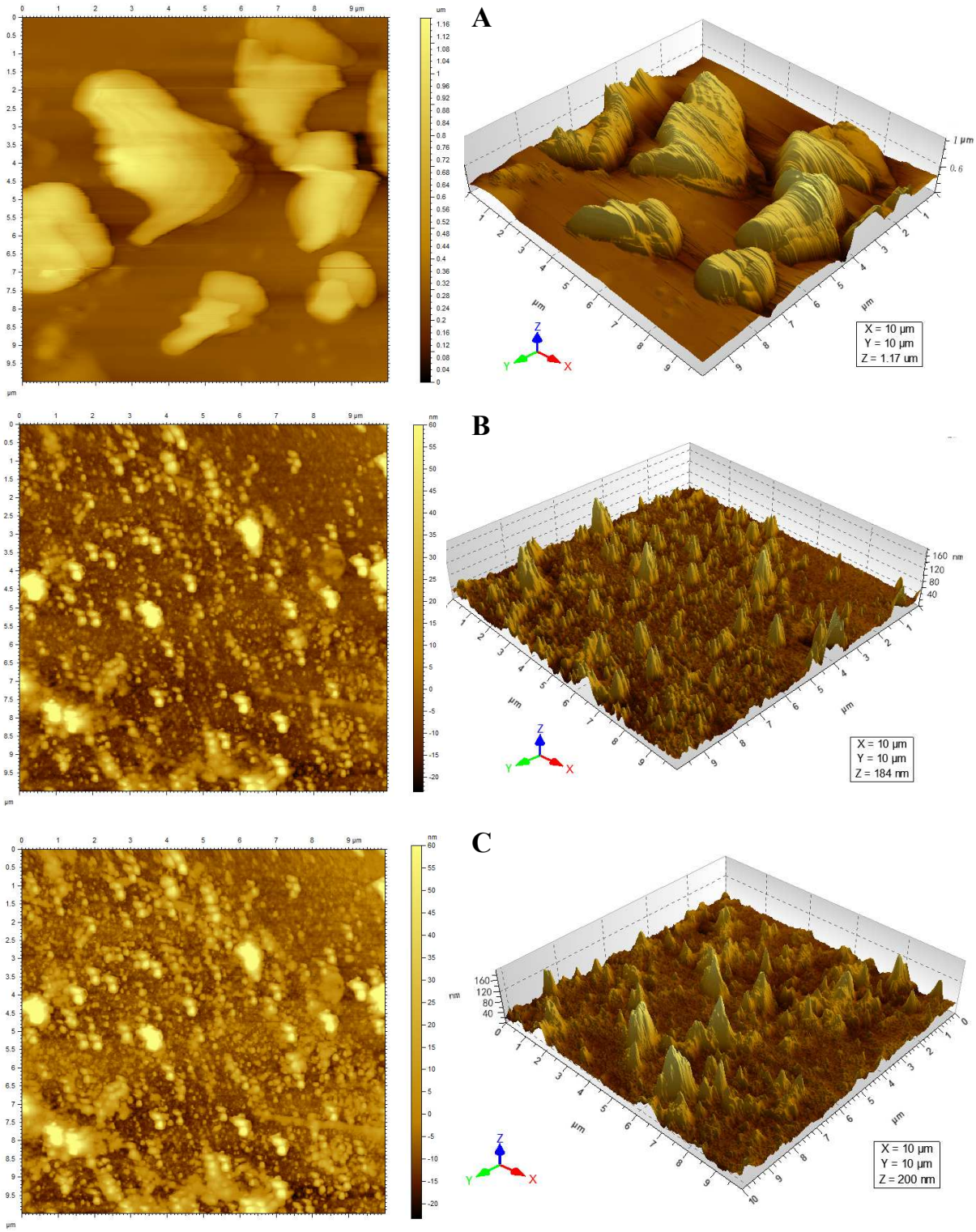

Fig. 5 AFM topographic images of antibodies immobilized on the gold surface. (A) APTES-modified crystal; (B) SPA-coated crystal; and (C) APTES + SPA modified crystal.